Interdecadal-decadal climate variability from multicoral oxygen isotope records in the South Pacific Convergence Zone region since 1650 A.D.

Braddock K. Linsley,[1] Peipei Zhang,[1] Alexey Kaplan,[2] Stephen S. Howe,[1] and Gerard M. Wellington[3]

Received 3 September 2007; revised 22 February 2008; accepted 27 March 2008; published 20 June 2008.

[1] In the South Pacific, interdecadal-decadal oceanic and atmospheric variability, referred to as the Interdecadal Pacific Oscillation (IPO), is most pronounced in the South Pacific Convergence Zone (SPCZ) salinity front region. Here we have used annual average oxygen isotope ($\delta^{18}O$) time series from five coral cores collected from Fiji and Tonga in this region to construct a Fiji-Tonga Interdecadal-Decadal Pacific Oscillation (F-T IDPO) index of low-frequency (>9 and <55 years) climate variability back to 1650 A.D. We first demonstrate the consistency between this F-T IDPO index and a mean sea level (MSL) pressure-based SPCZ position index (SPI) (1891–2000), thus verifying the ability of coral $\delta^{18}O$ to record past interdecadal-decadal climatic variations in this region back to 1891. The F-T IDPO index is then shown to be synchronous with the IPO index (1856–2000), suggesting that this coral-based index effectively represents the interdecadal-decadal scale climate variance back to 1650. The regularity of the F-T IDPO index indicates that interdecadal-decadal variability in the SPCZ region has been relatively constant over the past 350 years with a mean frequency of ~20 years (variance peaks near 11 and 35 years). There is a consistent antiphase correlation of the F-T IDPO index and the interdecadal-decadal components in equatorial Pacific coral $\delta^{18}O$ series from Maiana and Palmyra. This observation indicates that the eastward expansion (westward contraction) of the eastern salinity front of the Western Pacific Warm Pool (WPWP) occurs simultaneously (±<1 year) with the westward (eastward) shift of the SPCZ salinity front during positive IPO (negative IPO) phases. This is the same relationship observed during the phases of the El Niño Southern Oscillation.

Citation: Linsley, B. K., P. Zhang, A. Kaplan, S. S. Howe, and G. M. Wellington (2008), Interdecadal-decadal climate variability from multicoral oxygen isotope records in the South Pacific Convergence Zone region since 1650 A.D., *Paleoceanography*, *23*, PA2219, doi:10.1029/2007PA001539.

1. Introduction

[2] The South Pacific Convergence Zone (SPCZ) is a reverse oriented monsoonal low-pressure trough stretching from the Intertropical Convergence Zone (ITCZ) near the Solomon Islands to Fiji, Samoa, Tonga and farther southeast to French Polynesia (Figure 1). This region features a large sea surface temperature (SST) gradient and active low-level convergence. The low-level convergence of moisture leads to a persistent cloud band as well as showers and thunderstorms. Precipitation and convection within the band is seasonally dependent. Its equatorial portion, where it is connected to the ITCZ, is most active in the Southern Hemisphere summer, and the more southeasterly portion is most active during transition seasons of fall and spring. On interannual timescales, displacements of the SPCZ are relatively well known. During La Niña phases the SPCZ shifts southwestward and during El Niño phases the SPCZ shifts northeast toward Samoa [*Folland et al.*, 2002; *Gouriou and Delcroix*, 2002]. However, lower-frequency displacements are less well understood because of the lack of long-term instrumental records. *Folland et al.* [2002] have developed a SPCZ position index (SPI) from the monthly instrumental mean sea level (MSL) pressure differences between Suva, Fiji (18°9′S, 178°26′E) and Apia, Samoa (13°48′S, 171°47′W) from November to April during the period 1891–2000 (see Figure 2). The SPI was found to be closely correlated with the phase of the Interdecadal Pacific Oscillation (IPO), with the SPCZ displaced toward Fiji during negative phases of the IPO and toward Samoa during positive phases of the IPO [*Folland et al.*, 2002]. At lower frequencies, *Linsley et al.* [2006] have interpreted the secular trends in replicated coral oxygen isotope ($\delta^{18}O$) records from Fiji and Rarotonga as evidence that the SPCZ has been expanding southeast since the mid 1800s.

[3] At the southeastern edge of the SPCZ, oceanic circulation around the feature in conjunction with a positive precipitation-evaporation (P-E) balance in the SPCZ creates a salinity gradient in the ocean, with fresher and warmer waters of the western Pacific lying to the west of the salinity

[1]Department of Earth and Atmospheric Sciences, University at Albany, State University of New York, Albany, New York, USA.
[2]Lamont-Doherty Earth Observatory, Columbia University, Palisades, New York, USA.
[3]Department of Biology and Biochemistry, University of Houston, Houston, Texas, USA.

0883-8305/08/2007PA001539$12.00

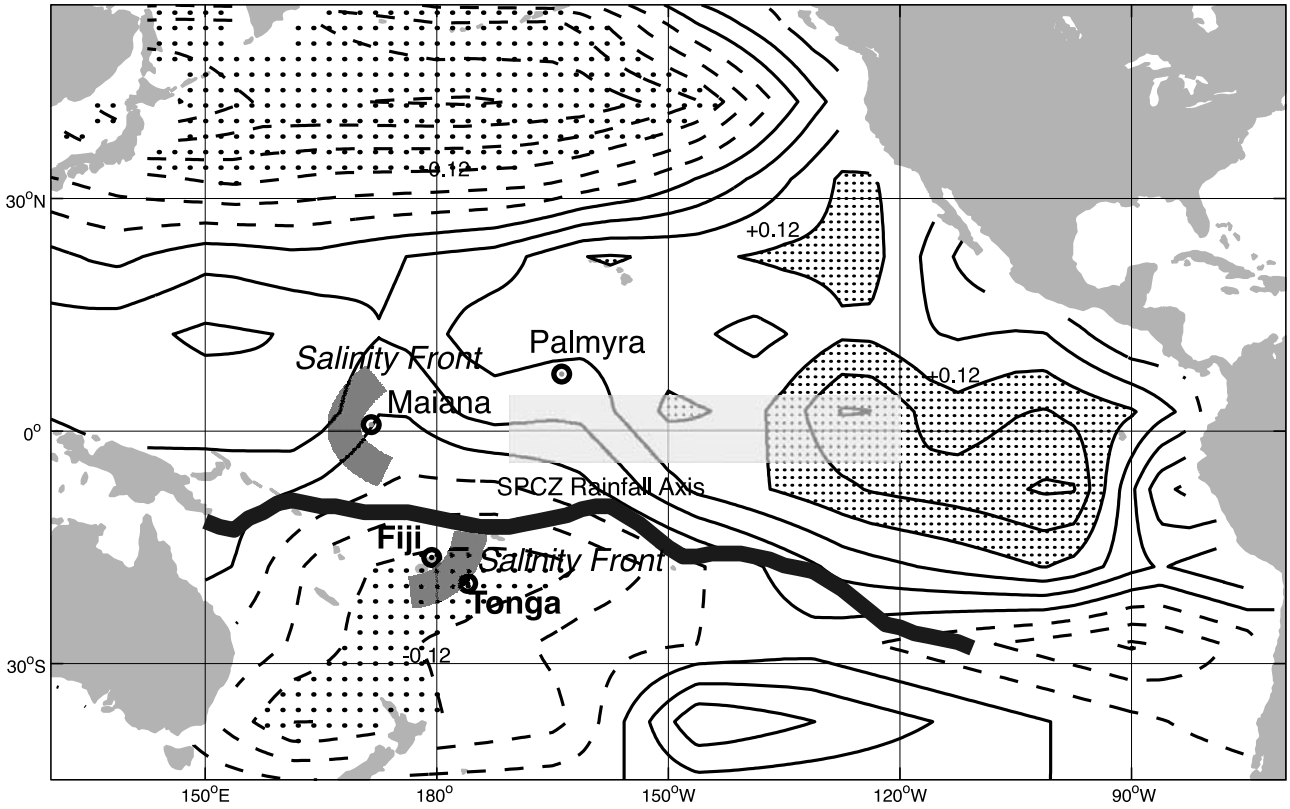

Figure 1. Location of Fiji, Tonga, Maiana, Palmyra, and the Nino 3.4 area (shaded box, 5°N–5°S, 120°–170°W) in relation to the South Pacific Convergence Zone salinity front near Fiji and Tonga, to the West Pacific Warm Pool salinity front near Maiana and to the spatial pattern of the IPO [*Folland et al.*, 2002]. Background contours show the IPO as a covariance map of the 3rd EOF of low pass-filtered SST anomalies for 1911–1995. The contour interval is 0.04°C, negative contours are dashed, values <−0.12°C sparsely stippled, and those >+0.12°C densely stippled. The maximum rainfall axis of the SPCZ for 1958–1998 is also shown as a thick black line. Figure modified from *Folland et al.* [2002].

front and cooler, saltier waters lying to the east [*Gouriou and Delcroix*, 2002] (see Figures 1 and 2). On interannual scales, when the SPCZ migrates northeastward (southwestward) during El Niño (La Niña) events, the salinity front simultaneously shifts northwestward (southeastward) [*Gouriou and Delcroix*, 2002; *Juillet-Leclerc et al.*, 2006; *Linsley et al.*, 2006]. On interdecadal timescales the SPCZ salinity front also migrates northwestward (southeastward) during the negative (positive) phase of the IPO (see Figure 1), e.g., westward during the late 1940s to mid 1970s and eastward after the mid-1970s [*Delcroix et al.*, 2007].

[4] In many studies, δ^{18}O series in corals have been shown to provide a unique record of past climatic variability because of (1) the precise dating provided by annual growth bands combined with δ^{18}O annual cycles and (2) the ability of coral skeletal δ^{18}O to record environmental changes [e.g., *Wellington et al.*, 1996]. However, limitations of using the coral δ^{18}O proxy include uncertainties both in the combined effects of SST and the δ^{18}O of seawater and in the effects of poorly understood potential biological artifacts such as inconsistent annual skeletal extension rates and calcification rates [*Lough*, 2004]. Skeletal diagenesis either via secondary calcification or dissolution can also be hard to detect [*Müller et al.*, 2001; *Hendy et al.*, 2007].

[5] Here we use a regional multicoral δ^{18}O series approach in an attempt to minimize potential biological or diagenetic artifacts and to increase the climate signal-to-noise ratio of the interdecadal-decadal δ^{18}O variability. The climatic significance of interdecadal-decadal modes in coral δ^{18}O time series is still under debate [e.g., *Jones et al.*, 1998; *Crowley et al.*, 1999; *Evans et al.*, 2000; *Linsley et al.*, 2004, 2006]. To examine the reliability of the coral-based δ^{18}O proxy in reconstructing interdecadal and decadal climate variability in the past, we isolated the interdecadal-decadal modes in five coral δ^{18}O time series in the SPCZ region (two from Fiji and three from Tonga) (Figure 2). Both island chains lie in an area of the South Pacific where the IPO is most pronounced (see Figure 1). *Folland et al.* [2002] demonstrated the equivalence of the IPO and the North Pacific derived Pacific Decadal Oscillation (PDO) index. In the South Pacific the IPO amplitude appears to be of similar magnitude to the El Niño Southern Oscillation (ENSO). Large uncertainties remain regarding the temporal and spatial coherence of

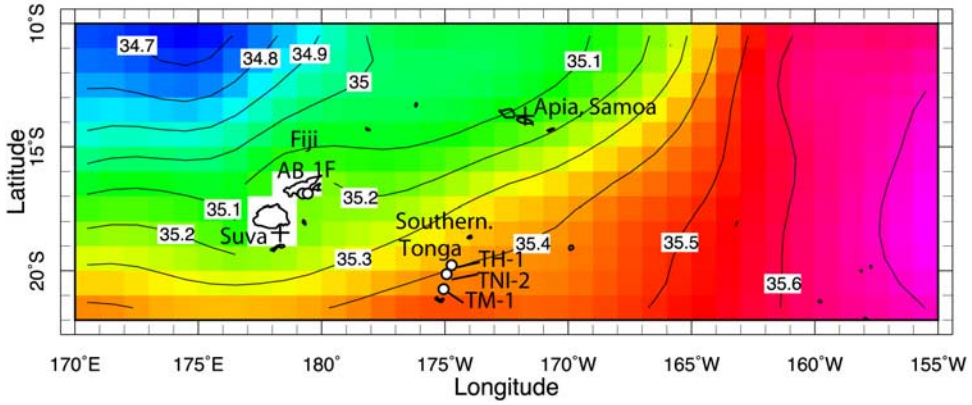

Figure 2. Study sites in Fiji and Tonga (black outlined circles) in relationship to annually averaged sea surface salinity (data from *Boyer et al.* [2002] and *Conkright and Boyer* [2002]) (contours in psu). The SPCZ-related sea surface salinity front can be seen aligned northeast-southwest across the study area. Plus signs mark Apia, Samoa, and Suva, Fiji. The difference in mean sea level pressure between these sites was used to define the SPCZ position index (SPI) [*Folland et al.*, 2002].

this interdecadal-decadal variability prior to ~1950 when instrumental data were less complete in coverage and are generally thought to be less reliable. Here we will show that the interdecadal-decadal variability extracted from the δ^{18}O series of five corals from Fiji and Tonga correlates with the SPI and IPO indices. This demonstrates the reliability of coral δ^{18}O from Fiji and Tonga as a climate proxy at interdecadal-decadal frequencies and establishes that a five coral δ^{18}O composite Interdecadal-Decadal Pacific Oscillation (IDPO) index back to 1650 A.D. documents past interdecadal-decadal climate oscillations.

2. Methods

2.1. Sampling and Chronology

[6] In November 2004 three *Porites lutea* coral colonies were drilled at Tonga on the islands of Ha'afera, Malinoa, and Nomuka Iki (Figure 2). At Ha'afera (19°56′S, 174°43′W), a large colony with a dead flat top but with live sides was cored (see Table 1). The colony was ~4 m high with ~1 m of water covering the top at low tide. Two coral cores TH1 Hole 4 (TH1–H4 hereafter) and TH1 Hole 5 (TH1–H5 hereafter) were collected from this colony. The 3.28-m-long core TH1–H4 was drilled from the dead top of the colony and the 67-cm-long core TH1–H5 was collected from the live side of the colony. As discussed below, TH1–H4 and TH1–H5 were spliced together using the timing of known El Niño events. At Malinoa (21°02′S, 175°08′W), just north of Nuku'alofa in southernmost Tonga, a 1.63-m-long core (TM1) was collected from a living colony in 6 m of water. At Nomuka Iki (20°16′S; 174°49′W) two useable cores were collected from a large living colony in 3.5 m of water (TNI2-H1, 4.03 m useable length; and TNI2-H3, 1.8 m useable length). Because of a bio-eroded zone from ~1 m to 1.68 m in TNI2-H1, TNI2-H3 was drilled to allow sampling around the bio-eroded zone by splicing the δ^{18}O record from H3 onto H1.

[7] The δ^{18}O data from the two Fiji *Porites lutea* cores (Fiji 1F and Fiji AB) used in this study were originally discussed by *Linsley et al.* [2004, 2006]. It should be noted that subsequent to publishing the Fiji core AB chronology by *Linsley et al.* [2006], we determined that a 2-year gap existed in this core (missing years 1727 and 1728) at a core break. For this current work we have inserted 2 years by interpolating between the adjacent annual average d180 values above and below the gap. *Bagnato et al.* [2004] evaluated the variability in a δ^{18}O time series (2001–1776 A.D.) generated from a *Diploastrea* coral core collected in the same bay as Fiji cores 1F and AB. *Diploastrea* skeletons extend at a rate that is 2–3 times slower than *Porites* in the same setting. Given the possible biological effects of this slower growth on skeletal geochemistry [*Pätzold*, 1984; *Bagnato et al.*, 2004] we have elected not to include this *Diploastrea* time series in our *Porites* δ^{18}O composite. In addition, if any nonclimatic

Table 1. List of Five *Porites lutea* Coral Cores Used to Develop the Composite Interdecadal-Decadal Pacific Oscillation Index[a]

Core	Years	δ^{18}O Sampling	Water Depth	Location	Latitude and Longitude
1F	1997–1780	Millimeter scale	10 m	Savusavu Bay, Fiji	16°49′S 179°14′E
AB	2001–1617	Millimeter scale	10 m	Savusavu Bay, Fiji	16°49′S 179°14′E
TH1	2004–1794	Millimeter scale and annually	1 m	Ha'afera, Tonga	19°56′S 174°43′W
TNI2	2004–1650	Millimeter scale and annually	3.5 m	Nomuka Iki, Tonga	20°16′S 174°49′W
TM1	2004–1837	Millimeter scale and annually	6 m	Malinoa, Tonga	21°02′S 175°08′W

[a]Description of Fiji cores (designated 1F and AB) were given by *Linsley et al.* [2004] and *Linsley et al.* [2006].

Table 2. Number of $\delta^{18}O$ Measurements for Each Tonga Core Studied Here and the Average Difference of Replicate $\delta^{18}O$ Measurements by Core[a]

Core	Number of Samples Analyzed	Average Difference of Replicates	Average $\delta^{18}O$ Value of NBS-19 Standard Analyzed Daily (n = number analyzed)
TH1–H4	522	0.036	−2.199 ± 0.031 (n = 135)
TH1–H5	192	0.039	−2.199 ± 0.031 (n = 135)
TM1	391	0.037	−2.195 ± 0.030 (n = 76)
TNI2-H1	889	0.056	−2.206 ± 0.034 (n = 152)
TNI2-H3	1306	0.047	−2.200 ± 0.038 (n = 218)

[a]The $\delta^{18}O$ results for the two Fiji cores have been previously reported [*Linsley et al.*, 2004, 2006].

(biological and/or digenetic) effects on skeletal $\delta^{18}O$ in each coral record used in the composite are independent and not related to each other, this nonclimatic signal will be minimized or canceled out by averaging multiple coral records, assuming the climatic signal preserved is the same for all corals used in the average. Since, in slow-growing corals like *Diploastrea*, the climatic versus nonclimatic components are not as well understood as they are in *Porites*, we decided not to include cores of any species of coral other than *Porites lutea*.

[8] All of the Tonga coral cores were cut into ~7-mm-thick slabs in the laboratory with a modified tile saw, cleaned and air-dried. The slabs were X-rayed (35 kV for 90 s) to reveal the density bands. All of the Tonga coral slabs were then cleaned with a high-energy (500 W, 20 kHz) probe sonicator in a deionized water bath for approximately 6 min and air-dried. As previously described [*Linsley et al.*, 2004, 2006] the Fiji coral core 1F and AB slabs were cut to a thickness of 6 mm and then cleaned in a 160 W ultrasonic bath prior to sampling and analysis. Dry slabs were sampled using a low-speed microdrill with a 1-mm-diameter diamond drill bit parallel to corallite traces along growth axes (as identified in the X-radiographs). Each Tonga core was sampled at 1-mm intervals through the top ~30 years, by excavating a 4–5-mm-wide (perpendicular to the growth axis) and 2–3-mm-deep groove in the coral slabs. Below the top ~30 years of growth in the Tonga cores a technique of annual scale sampling was used (described below). In order to sample continuously along the growth axes, the sampling track was purposely shifted from one growing axis to another as sampling progressed down core. Shifting the sampling track was also necessary to bypass possible gaps caused by irregular core breaks (see example X-ray collage in Figure S1 in the auxiliary material).[1] In these cases, all of the shifts were made along a distinct density band to avoid any temporal hiatus in our data. The Fiji cores were sampled at 1-mm intervals from the top to the bottom of each core.

[9] Approximately 100 μg of coral powder in each sample was dissolved in 100% H_3PO_4 at 90°C in a MultiPrep sample preparation device and the generated CO_2 gas was analyzed by a Micromass Optima gas source triple-collector mass spectrometer at the University at Albany, State University of New York Stable Isotope Ratio Mass Spectrometry Laboratory. Table 2 lists the number of samples analyzed from each Tonga core, the average difference between replicate samples and the average difference of the NBS-19 standards run for each core. Approximately 13% of the 3,300 Tonga coral samples were analyzed in duplicate. All data are expressed in the conventional delta notation as per mil deviations relative to Vienna Peedee Belemnite (VPDB).

[10] For the most recent three decades of cores TH1–H4, TH1–H5, TM1, and TNI2-H3, the chronologies are based on the reconstructed annual cycles in millimeter-scale $\delta^{13}C$ and $\delta^{18}O$ data with the warmest time, based on annual $\delta^{18}O$ minima, set as March. The 1974–1975 La Niña, 1971–1972 La Niña, 1964–1965 El Niño, and 1955–1957 La Niña events were set as control points to determine the age of TH1–H4 (the same colony as TH1–H5, but dead on the top). La Niña events result in warmer and lower salinity conditions in Fiji and Tonga (opposite from the equatorial Pacific) that lower coral $\delta^{18}O$, while during El Niño phases, locally cooler and saltier conditions result in higher coral $\delta^{18}O$ values. Figure 3 shows the millimeter-scale $\delta^{18}O$ results from cores TH1–H4, TH1–H5 and TNI2-H3 to illustrate the match of the interannual $\delta^{18}O$ changes with known ENSO events. We added TH1–H5 on top of TH1–H4 (the overlapping part was averaged) and named the combined time series data set spanning 1794–2004 TH1.

[11] Below the millimeter-scale sampling, we have utilized an annual-average sampling method, which is based on the annual density cycles identified by using X-ray radiographs and ultraviolet light. Sampling was done along the maximum growth axis as with the millimeter-scale sampling, but only one continuous sample was drilled through each high density band-low density band couplet (~8–17 mm long, depending on the coral extension rates). Powder from each annual accretion drilling was well mixed and its $\delta^{18}O$ value was taken as 1-year average value of the corresponding year. Millimeter sampling was applied in intervals where the density bands were not clear enough to identify the annual growth increments. Unlike the millimeter-scale sampled Fiji cores (Fiji 1F [*Linsley et al.*, 2004] and Fiji AB [*Linsley et al.*, 2006]), whose annual average $\delta^{18}O$ values were derived from all the data points between the two most negative $\delta^{18}O$ values of each year (March), the annual average $\delta^{18}O$ values from the annual scale drilling of the Tonga cores are not necessarily 12-month averages. In the Tonga cores, although most of the dense bands appear right before the warmest time in each year (January–February), there are exceptions that cause differences in time spans of some years. Instead of an integrated 1-year cycle, several months could be missed and added to the year before or after. However, as discussed below, the

[1]Auxiliary materials are available in the HTML. doi:10.1029/2007PA001539.

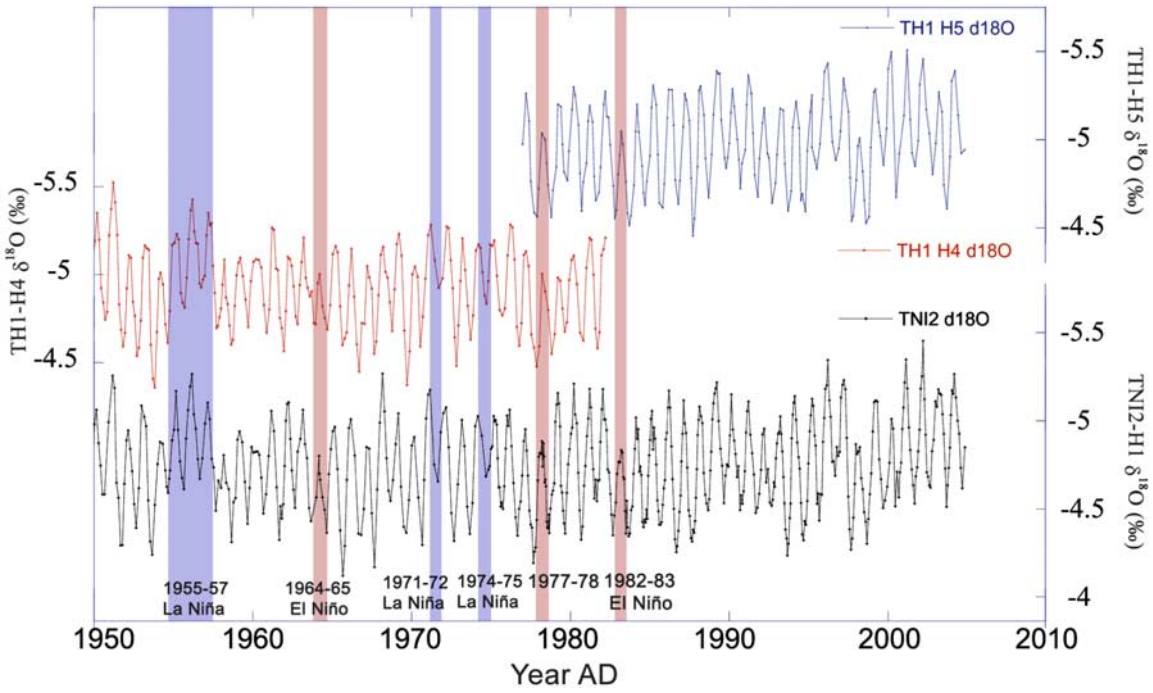

Figure 3. The plots of (top) TH1–H5, (middle) TH1–H4, and (bottom) TNI2-H1 over the period of 1950–2004 illustrate the match of the annual cycles during El Niño events highlighted in brown and La Niña events highlighted in blue. The δ^{18}O data from TH1–H5 was spliced onto the top of TH1–H4 (with dead top) on the basis of cross-dating with data from core TNI2 and by aligning El Niño and La Niña events (also see Figure S1 for X-ray collage of the TH1 cores).

similarity of the resulting modes in different frequencies among the five coral cores confirms the practical reliability of our sampling technique.

2.2. Statistical Analysis

[12] Following the approach of *Vautard and Ghil* [1989] and *Vautard et al.* [1992] we performed Singular Spectrum Analysis (SSA) of the annually averaged coral δ^{18}O time series. We used an SSA program written by E. Cook (Lamont-Doherty Earth Observatory) for this analysis. SSA has been previously applied to coral time series [e.g., *Dunbar et al.*, 1994; *Linsley et al.*, 1994, 2000; *Charles et al.*, 1997]. SSA is a fully nonparametric analysis technique based on principal component analysis that decomposes time series into several significant frequency components. It uses M-lagged copies of a centered time series to calculate eigenvalues and eigenvectors of their covariance matrix. The sampled time series X of length N is used to fill in a $(N - M + 1) \times M$ matrix by taking as state vectors the consecutive sequences $Z_n = (X_n, X_{n+1} \ldots X_{n+m-1})$ from $n = 1$ to $N - M + 1$. Variable M is called the embedding dimension or window width. Frequency separation increases as M increases, whereas statistical significance of correlations decreases. The value of M should not exceed $N/3$ [*Vautard et al.*, 1992]. Reconstructed components (RCs) are then calculated which allow a unique expansion of the signal into a sum of the different components. A detailed description of this technique and its paleoclimate application is given by *Vautard and Ghil* [1989] and *Vautard et al.* [1992].

[13] Varying window widths were applied over a reasonable range to the annually averaged δ^{18}O time series data of each core. The stable features of the eigenvectors were evaluated and an appropriate M value was selected to resolve the IPO band (~9–55 years) which was the focus of this research. Since the time series are of different lengths, M varied between cores. The SSA results presented here are based on the following M settings: Fiji 1F with M = 40 (N = 216), Fiji AB with M = 55 (N = 384), Tonga TH1 with M = 30 (N = 212), TNI2 with M = 50 (N = 355) and TM1 with M = 40 (N = 168).

3. Results

[14] An offset in mean δ^{18}O value previously observed for several other replicated coral records [*Tudhope et al.*, 1995; *Linsley et al.*, 1999, 2004, 2006; *Cobb et al.*, 2003] also exists in some of the five corals studied here. The 20th century mean values for annually averaged δ^{18}O are −4.64‰ for core AB, −5.06‰ for core 1F, −4.88‰ for core TH1, −4.70‰ for core TNI2, and −4.43‰ for core TM1. In the three Tonga corals, the offsets could be due to mean SST or sea surface salinity (SSS) differences between sites TH1, TNI2 and TM1. In the case of the two Fiji cores, the offset is 0.42‰. These *Porites* colonies are growing in the same setting at the same water depth within 200 m of each other in Savusavu Bay and this difference in mean δ^{18}O could be due to a difference in the disequilibrium δ^{18}O offset. Given the uncertainty of the significance of this offset from equilibrium δ^{18}O, we have "centered" each of

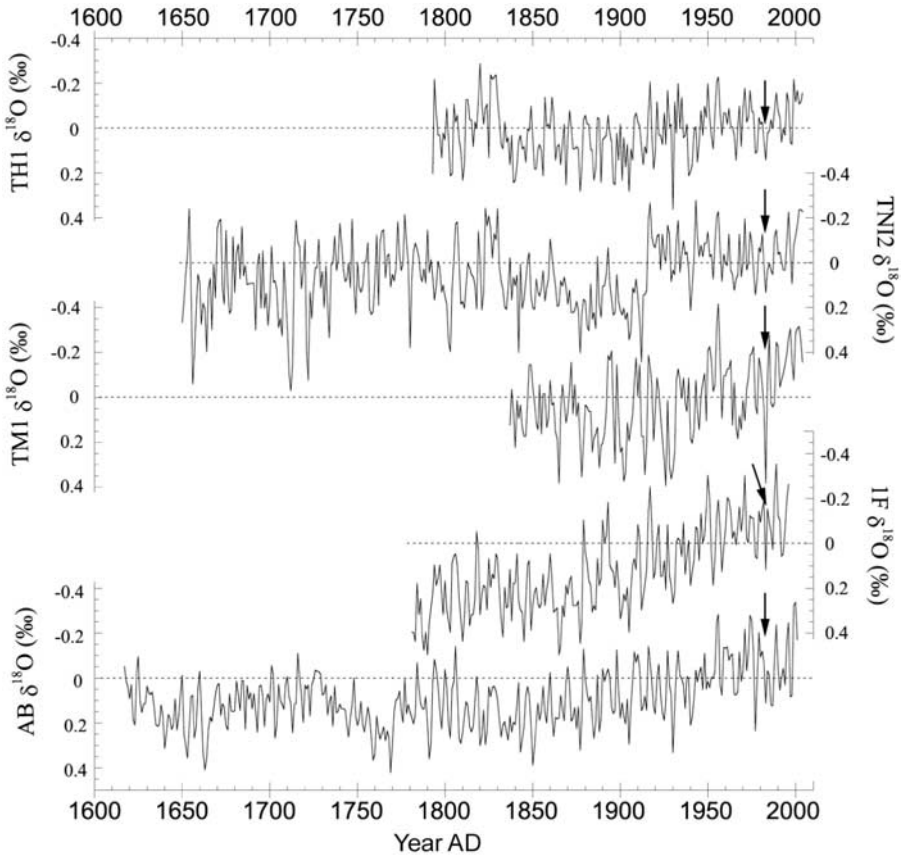

Figure 4. Annually averaged δ^{18}O data of the five corals from Fiji and Tonga with the 20th century mean values removed. The black arrows show the 1982–1983 El Niño event. The δ^{18}O (‰) scale is the same for all five corals.

the five coral δ^{18}O series by subtracting the twentieth century mean δ^{18}O value of each core in order to facilitate comparison of the δ^{18}O time series. Centered δ^{18}O series for the five cores are shown in Figure 4. Since all five colonies are composed of the same species of coral and are from a relatively small area, they should contain common variance due to regional climatic variability.

[15] Because these are annual averaged δ^{18}O time series, we expect to see small differences between the amplitude of δ^{18}O "events" within any given year. For example, the 1982–1983 El Niño event (marked by arrows on Figure 4) resulted in a simultaneous increase in coral δ^{18}O values in all five corals. The difference in δ^{18}O amplitude of this El Niño event (and other events) in each core may be in part related to uncertainties associated with measuring δ^{18}O in 1-year increments. These include analytical uncertainties (at least ±0.045‰, see Table 2) and errors produced by the inevitable mismatches between the length of the sample increment and the actual length of the annual cycle (probably at least ±0.1‰ based on amplitude of SST annual cycle). The total uncertainty could easily be ±0.15‰. There is also the possibility of biological effects, such as short-term bleaching affecting one coral colony but not others. This may be the case for the 1982–1983 El Niño that resulted in a ~0.15‰ increase in δ^{18}O in the Tonga cores TH1 and TNI2 and in the Fiji cores 1F and AB, but which caused an even more pronounced 0.5‰ increase in δ^{18}O in Tonga core TM1.

[16] Four out of the five corals show a clear, gradual trend toward warmer and fresher conditions since the late 1800s (Figure 4), which probably indicates a southeastward shift of the SPCZ and associated SSS front [*Linsley et al.*, 2006]. The only exception is TNI2 which records a less obvious trend that is partly obscured by an abrupt 0.3‰ decrease in δ^{18}O between 1915 and 1916. We believe this "jump" is the result of an unknown biological or diagenetic effect and/or the possible tectonic shifting of water depth at the coral site (the active Tonga trench is nearby), since the synchronous δ^{13}C values are normal and there did not exist any known climatic event that could change the temperature and/or salinity to cause a 0.3‰ drop in δ^{18}O.

[17] We performed SSA to quantify the variance in the annual-averaged coral δ^{18}O time series from each core. For the coral δ^{18}O series analyzed in this study, we separated the oscillatory components into three groups: trend, interdecadal-decadal, and ENSO. The ENSO band was set to frequencies ranging between 3 and 8 years. This frequency cut-off for ENSO has been widely applied and is based on the recurrence interval of recent El Niño events. The SSA results for Core TH1 also show biennial components

that we did not include in the ENSO band. The mean frequencies of the interdecadal-decadal band were set between ~9 and ~55 years. Below, we will refer to this band as the Interdecadal-Decadal Pacific Oscillation (IDPO). Since the IDPO actual frequency in the Pacific is still under debate and has previously been defined as the quasi-decadal oscillation [*Mann and Park*, 1994], the bidecadal oscillation [*Minobe et al.*, 2002], and the PDO/IPO, we took a conservative approach and elected not to subdivide this component. Thus the IDPO-band includes all oscillations with frequencies lower than ENSO and higher than the secular trend. Here we defined the secular trend as frequencies >75 years. We note that in the five coral δ^{18}O time series no oscillatory components have mean frequencies between 55 and 75 years, thus 75 years appears to be a logical frequency cutoff to separate the interdecadal variability from the secular trend.

[18] SSA of the Tonga and Fiji coral δ^{18}O records indicates that between 13 and 38% of the variance in each annual-averaged time series is in the IDPO band with mean periods between ~9 and ~55 years. The percent variance of IDPO or ENSO bands varies in each core with core TM1 having the most pronounced IDPO variance at 38.4%, which is about twice as large as in the other cores. Besides the exceptionally large variance, the IDPO of TM1 exhibits a perceptibly different amplitude pattern from the other four cores. A possible explanation is that TM1 (near Nuku'alofa, in southern Tonga) lies at the boundary between two climate regions [*Salinger et al.*, 1995] and is not only influenced by southeast trade winds but also by southern westerlies in the anticyclonic belt, while the four other corals are mainly affected by southeast trade winds. This coral is also the only one to contain significant fungal pigments [*Priess et al.*, 2000].

4. Discussion

4.1. Temperature Versus Salinity Contribution to δ^{18}O Variability

[19] Analysis of instrumental SST, sea surface salinity (SSS), and precipitation records in the SPCZ-SSS front region beginning in 1976 indicate that each contains an interannual signal that correlates with the Southern Oscillation Index (SOI) and ENSO [*Gouriou and Delcroix*, 2002]. In this region the amplitudes of the interannual signals in SST and precipitation are an order of magnitude less than the amplitude of the seasonal cycle, whereas for SSS, the interannual signal of 1–1.5 practical salinity units (psu) is double the amplitude of the seasonal signal [*Gouriou and Delcroix*, 2002]. At both Fiji and Tonga instrumental 2° × 2° latitude-longitude gridded SST [*Reynolds and Smith*, 1994] and 2° × 10° latitude-longitude gridded SSS [*Gouriou and Delcroix*, 2002] records reveal that each site has a pronounced seasonal SST cycle of 4°–5°C and a weak seasonal SSS cycle. On interannual timescales the opposite takes place, a weak SST signal of 1°–2°C and a larger 1 to 1.5 psu SSS signal (Figure 5).

[20] Since it is known that coral skeletal δ^{18}O is primarily related to water temperature and δ^{18}O of seawater, we expected to see influences of both parameters in these coral δ^{18}O series. *Linsley et al.* [2006] showed that when analyzed at a resolution of ~10 samples per year, the Fiji coral δ^{18}O signal is strongly modulated by the 4–5°C annual SST cycle, with interannual variability predominantly driven by SSS. For both Fiji and Tonga the seasonal δ^{18}O range of 0.8–1.0‰ is close to that expected for the 4°–5°C annual SST cycle [*Epstein et al.*, 1953; *Dunbar et al.*, 1994; *Wellington et al.*, 1996]. Interannual coral δ^{18}O variability appears to be largely the result of the 1–1.5 psu irregular interannual SSS cycle and the advection of the SSS front in response to ENSO.

[21] Figure 5 compares Tonga cores TH1, TNI2, and TM1 and Fiji cores 1F and AB annual-averaged δ^{18}O data to annual-averaged SSS from *Gouriou and Delcroix* [2002] and annual SST anomaly from the Hadley Center Sea Ice and Sea Surface temperature database (HadISST1). Correlation coefficients (r value) between annual-averaged coral δ^{18}O and SSS over the interval from 1976 to 2000 are 0.61 for Tonga core TH1, 0.52 for Tonga core TNI2, 0.62 for Tonga core TM1, 0.66 for Fiji core 1F and 0.71 for Fiji core AB (average 5 coral versus SSS r value = 0.62). Correlation coefficients between annual-averaged δ^{18}O and SST during 1870 to 1996 are −0.44 for Tonga core TH1, −0.46 for Tonga core TNI2, −0.41 for Tonga core TM1, −0.54 for Fiji core 1F and −0.64 for Fiji core AB (average 5 coral versus SST r value = −0.50). Assuming that the relationship between coral δ^{18}O and SST is −0.21‰/°C (−0.17 to −0.23‰/°C is the common range of coral δ^{18}O-SST calibrations [*Epstein et al.*, 1953; *Dunbar et al.*, 1994; *Gagan et al.*, 1994; *Wellington et al.*, 1996]), the 1°C interannual range of annual SST of both Tonga and Fiji from the HadISST1 during 1976–2000 contributes ~0.21‰ to the change in coral δ^{18}O in this time interval. Subtracting this 0.21‰ SST portion from the total coral δ^{18}O range (~0.5‰) during the same period of time results in a residual of ~0.3‰. The magnitude of the "residual" is in accord with the interannual 1–1.2 psu range based on the 0.27 to 0.45‰/psu range between $\delta^{18}O_{seawater}$ and SSS found for the equatorial western Pacific and South Pacific [*Fairbanks et al.*, 1997; *Morimoto et al.*, 2002; *LeGrande and Schmidt*, 2006]. We realize that the 0.27‰/psu relationship derived from the equatorial Pacific by *Fairbanks et al.* [1997] may be conservative and underestimate the amplitude of SSS variability for a given coral δ^{18}O change in this region. In the South Pacific, a 0.45‰/psu relationship was derived from limited data [*LeGrande and Schmidt*, 2006]. Using this relationship the residual ~0.3‰ coral δ^{18}O signal would reflect a 1.5 psu SSS change which is supported by the instrumental salinity data (see Figure 5).

[22] ENSO event and IPO phase effects on SST and $\delta^{18}O_{seawater}$ in this region result in additive effects on coral δ^{18}O. For example, during El Niño events and/or positive phases of the IPO index, locally cooler and saltier conditions increase coral δ^{18}O at Fiji and Tonga. The opposite occurs during La Niña events or negative IPO intervals. Since greater precipitation, advection of lower salinity water, and warmer temperatures (or drier/saltier conditions with cooler temperatures) occur together in the study area [*Folland et al.*, 2002], their effects should be additive on coral δ^{18}O. Thus, we interpret coral δ^{18}O variability in this

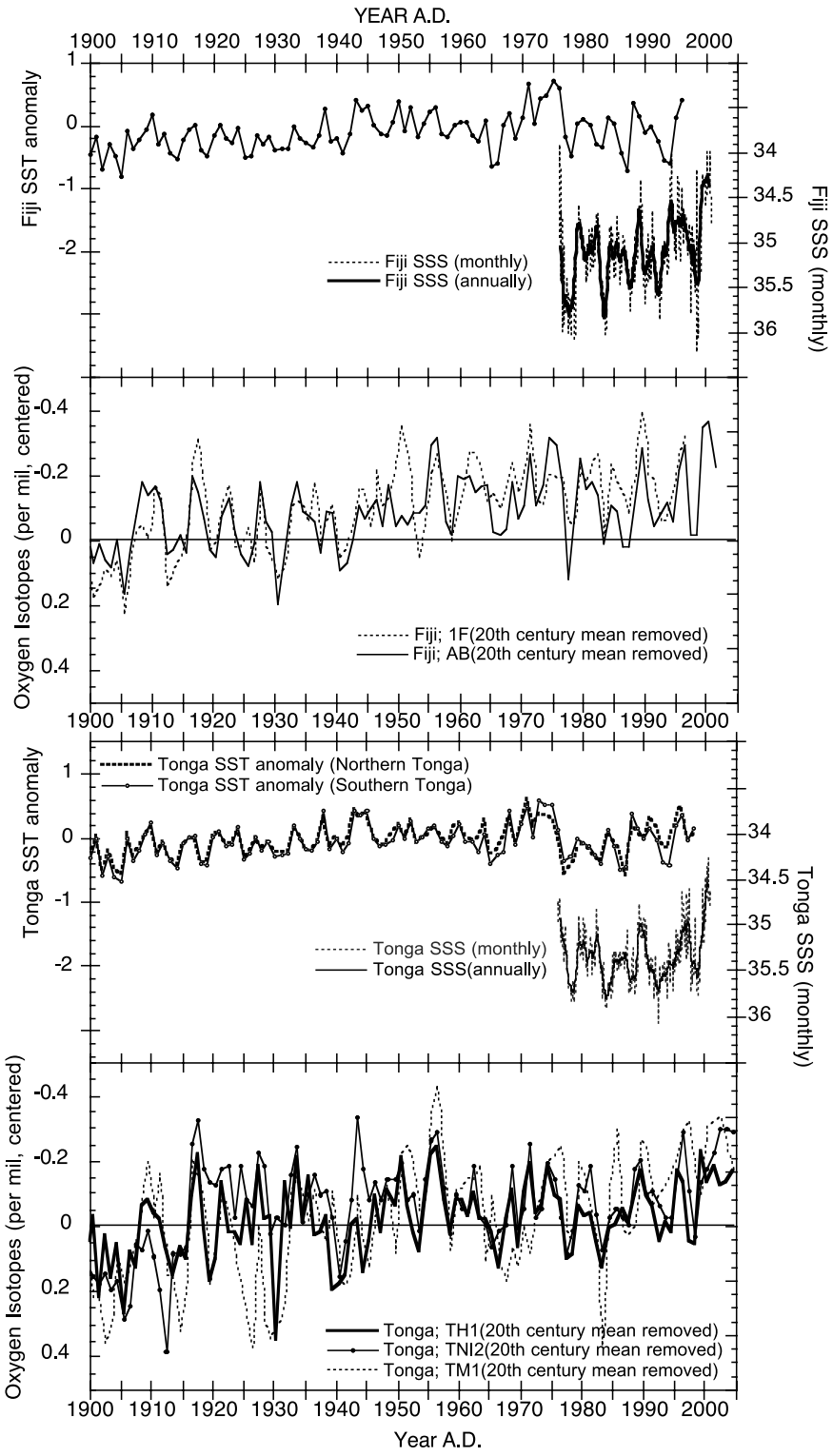

Figure 5. The relative contribution of SST and SSS changes to the coralline $\delta^{18}O$ variance in (top) Fiji and (bottom) Tonga. The annual SST data back to 1900 is from the HadISST1. Note that there are data from two regions in Tonga (northern Tonga and southern Tonga). Regional SSS data back to 1976 is from *Gouriou and Delcroix* [2002]. The SST (°C) and $\delta^{18}O$ (‰) were plotted on a 0.2‰/°C scale and the SSS (psu) and $\delta^{18}O$ (‰) were plotted on a 0.3‰/psu scale so that the relative contributions to $\delta^{18}O$ variability can be assessed (see text).

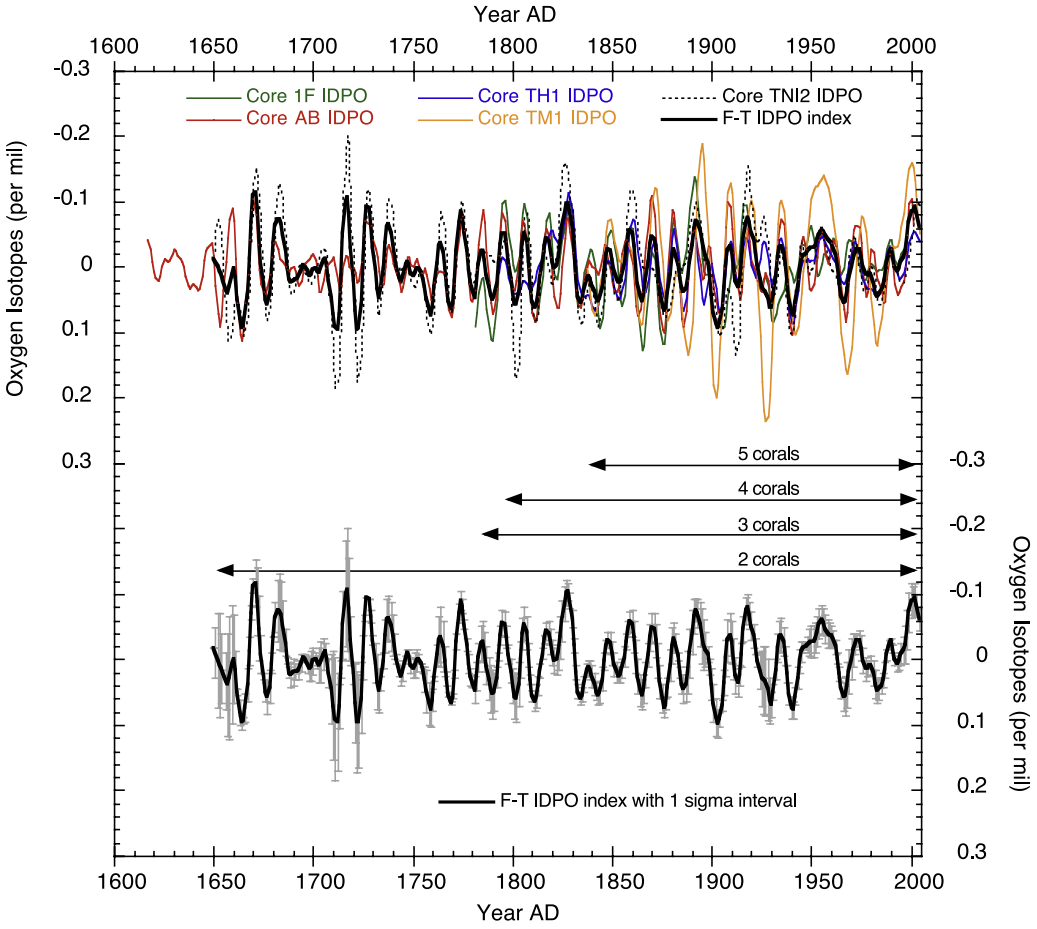

Figure 6. (top) IDPO signals of the five coral δ^{18}O series from Fiji and Tonga (thin colored lines) filtered by SSA, from which the average F-T IDPO index was created (thick black line). Labeled arrows indicate the number of corals whose spectra were included in the average IDPO index during various time intervals. (bottom) The F-T IDPO index shown with 1σ unbiased uncertainty envelop (see text).

region as an index of ENSO or the IPO/PDO without separating the effects of SST and SSS.

4.2. Fiji-Tonga Interdecadal-Decadal Pacific Oscillation Index

[23] Although the five coral cores were collected from a relatively small area (5°–6° latitude-longitude) along the salinity front at the southeast boundary of the SPCZ, the colonies grew in water of different depths in different lagoon/fore-reef settings. TH1 was collected in an isolated lagoon in 1 m water. TNI2 was collected from a colony in 3.5 m of water in a well-flushed passage. TM1 grew more slowly (~4–12 mm/a (where a is years)) than the other cores (~7–15 mm/a) and contained residue pigments along the density bands from fungal growth [*Priess et al.*, 2000]. Fiji Core AB [*Linsley et al.*, 2006] and Fiji core 1F [*Linsley et al.*, 2004] were collected at 10 m depth within 200 m of each other in Savusavu Bay.

[24] Despite various biological and unknown effects in these diverse settings that could potentially influence the skeletal δ^{18}O, we find that once the δ^{18}O series are corrected for differences in disequilibrium offset (as shown by *Linsley et al.* [1999]), the annually averaged δ^{18}O series contain common variance that can be attributed predominantly to climate variability. The IDPO variance (periods between ~9 and ~55 years) isolated from the δ^{18}O data of these five corals by SSA align reasonably well with each other back to 1650 (Figure 6). We argue that the reproducibility of the timing of the summed interdecadal and decadal components in the multicoral δ^{18}O series demonstrates an environmental origin for this mode of δ^{18}O variability despite the variations in amplitude observed in some intervals. The five coral Fiji-Tonga δ^{18}O series are from a region with a common climatic forcing related to the SPCZ and associated changes in SST and SSS [e.g., *Salinger et al.*, 1995; *Folland et al.*, 2002]. *Folland et al.* [2002] identified this region of the southwest Pacific as a "center of action" for the PDO/IPO. Therefore we developed a Fiji-Tonga IDPO index from the five coral δ^{18}O series we have generated.

[25] To obtain the index we calculated an average of interdecadal-decadal variability from all five corals and the 1σ error (see below and Figure 6) and term the result

Table 3. Correlation Coefficients (R Values) Between the Fiji and Tonga Coral δ^{18}O IDPO Indices[a]

	Tonga, TNI2	Tonga, TM1	Fiji, 1F	Fiji, AB
Tonga, TH1	0.67	0.35	0.47	0.55
Tonga, TNI2		0.23	0.49	0.37
Tonga, TM1			0.24	0.53
Fiji, 1F				0.45

[a]The low correlation between TNI2 and AB may be due to their inconsistency during ~1750–1760 and ~1700–1720.

the Fiji-Tonga Interdecadal-Decadal Pacific Oscillation (F-T IDPO) index. The calculation of the index and its 1σ standard error was performed as follows.

[26] At each year t there are $n(t)$ records $x_1(t)$, $x_2(t)$. . ...$x_{n(t)}$ (t) available.

[27] The index itself is computed as their mean

$$\bar{x}(t) = \frac{1}{n(t)} \sum_{i=1}^{n(t)} x_i(t). \quad (1)$$

[28] While its standard error is computed as

$$e(t) = \frac{\sigma(t)}{\sqrt{n(t)}}, \quad (2)$$

where $\sigma(t)$ is unbiased estimate of the standard deviation of all records available for the year t, computed from

$$\sigma^2(t) = \frac{1}{n(t) - 1} \sum_{i=1}^{n(t)} (x_i(t) - \bar{x}(t))^2. \quad (3)$$

[29] The correlation coefficients of the IDPOs for all of the five cores are listed in Table 3. TM1 is least correlated with other cores. This could be due to its more southerly location between two different climatic zones [*Salinger et al.*, 1995] as previously mentioned and may mean that TM1 contains climatic information from both regions. However, we note that removing TM1 from the index does not modify our composite average significantly.

[30] Potential chronological errors (1–2 years) in the δ^{18}O series may reduce the alignment (and r values), but chronological error is not likely to occur in all five cores in the same period of time and would not modify the five coral composite greatly. Furthermore, ENSO band (~3–8 years) variability in each coral δ^{18}O series was used to double check the accuracy of the chronologies (not shown here), and the alignment of the ENSO band between the five corals supports the reliability of our chronologies back to at least 1715 A.D. We do note ENSO band offsets between Fiji AB and Tonga TNI2 from 1715 to 1700 A.D. and from 1650 to 1660 A.D. (not shown), which probably are related to variations in interannual scale chronology. One motivation for developing a Fiji-Tonga IDPO index from multiple coral cores is to minimize the potential chronological errors and to reduce potential biological or diagenetic artifacts that can affect individual δ^{18}O series, [*Linsley et al.*, 1999; *Lough*, 2004; *Hendy et al.*, 2007]. We expect the F-T IDPO index to be more representative of interdecadal-decadal climatic variability in this region than any one of the five δ^{18}O series alone.

[31] In dendroclimatology, the expressed population statistic (EPS) is used to determine the number of records (N) required to produce an average (composite) with an acceptable signal-to-noise ratio for the calculated mean interseries correlation coefficient. *Wigley et al.* [1984] described the EPS. For dendroclimatology, the acceptable EPS is often set subjectively to $\geq$0.85 [*Wigley et al.*, 1984; *Briffa*, 1995]. *Delong et al.* [2007] described the application of the EPS approach to multiple subannual resolution coral Sr/Ca records from New Caledonia. They found an interseries correlation coefficient of 0.66 for annual averaged Sr/Ca data and concluded that for their data an $N = 3$ generates an EPS > 0.85. For the more regionally spread Fiji-Tonga corals, annual averaged δ^{18}O has a mean interseries correlation coefficient of 0.43 with all 5 corals, and 0.49 if we exclude core TM1 (Table 3). This indicates an EPS of ~0.7–0.75. Using the EPS approach this would suggest that we need ~2 more annual averaged δ^{18}O records from this region to generate an EPS > 0.85. Using our approach described above we find an average unbiased estimate of the standard deviation of the 5 coral δ^{18}O series is ±0.022‰ and that adding two more 200 or more year δ^{18}O series to our index would reduce the error in the IDPO index by (square root(7/5) − 1) * 100% = 18%. Thus, although additional δ^{18}O series would improve the index, the current 5 coral composite index has significantly increased the signal-to-noise ratio for the interdecadal-decadal band and allows us evaluate this low amplitude but important climate mode over time.

[32] The coherence between this five coral δ^{18}O IDPO composite and the SPI [*Folland et al.*, 2002] supports the reliability of this coral δ^{18}O-based IDPO index and the method of SSA deconvolution to reconstruct interdecadal to decadal scale climate changes in this region (Figure 7a). The correlation coefficient between the 3-year smoothed SPI and F-T IDPO is 0.39. Note that the SPI combines both ENSO and IDPO variances [*Folland et al.*, 2002]. The antiphase correlation of the SPI (Figure 7a), but not of the IPO (Figure 7b) in the most recent 10 years may be due to the anomalous El Niño activity during this time period (J. Salinger, personal communication, 2007). The relatively low R value may be caused by the ENSO component in the SPI that is excluded from the F-T IDPO index. Positive SPI values indicate a northeast displacement of SPCZ toward Apia (Samoa), creating cooler and saltier conditions in the study area (Fiji and Tonga) as the SSS front shifts to the west. This is in accord with times of more positive coral δ^{18}O in the F-T IDPO index. The consistency between the two indices, one oceanic and one atmospheric, confirms the climatic origin of the IDPO signal isolated in our five coral composite index and the synchronous IDPO-scale oceanic and atmospheric changes in this area.

[33] To evaluate the five coral composite IDPO index further, we also compare it with the IPO index of *Folland et al.* [2002], which is defined as the third Empirical Orthogonal Function (EOF) of 13-year low pass-filtered Pacific

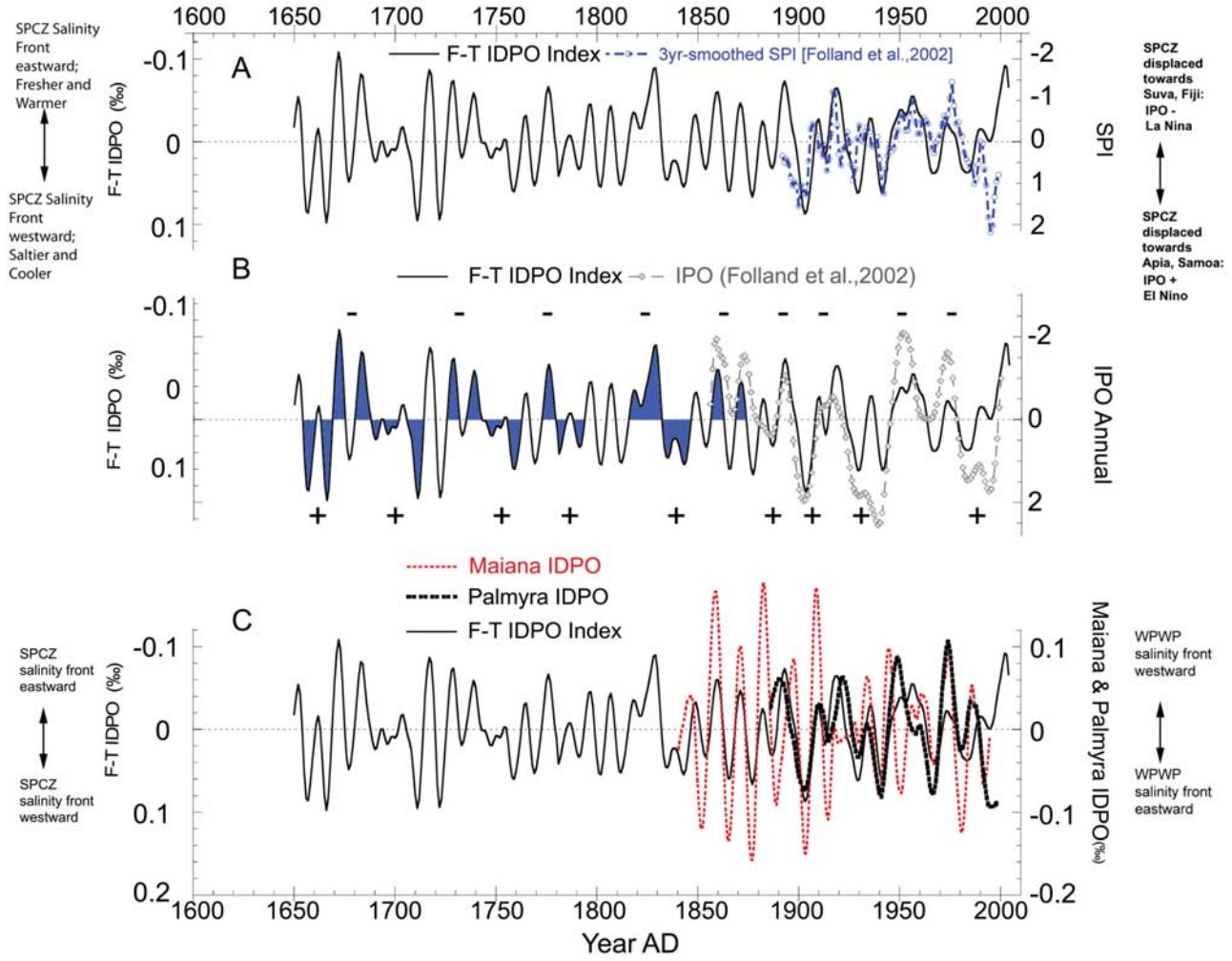

Figure 7. (a) The alignment between the F-T IDPO index and SPI [*Folland et al.*, 2002]. (b) The F-T IDPO index compared with the IPO index [*Folland et al.*, 2002]. The colored areas show the IPO phases revealed by the F-T IDPO index back to 1650 A.D. Plus signs indicate positive IPO phases, and minus signs indicate negative IPO phases. The IDPO phase changes are coherent with the instrumentally derived IPO and SPI indices. (c) F-T IDPO with two coral δ^{18}O series from the equatorial Pacific, both filtered by SSA to isolate the IDPO band. Note that the scale of the right-hand *y* axis of the Maiana [*Urban et al.*, 2000] and Palmyra [*Cobb et al.*, 2001] δ^{18}O series have been reversed for easier comparison with the left-hand *y* axis of the F-T IDPO index.

SST over the period 1911–1995. The IPO is highly correlated with the PDO index for the North Pacific, and *Folland et al.* [2002] suggested that the IPO could be regarded as the Pacific-wide manifestation of the PDO. The consistency between the F-T IDPO index and the IPO (Figure 7b) indicates that the interdecadal to decadal scale displacement of SPCZ shown by F-T IDPO is also related to the IPO.

4.3. Time Evolution of the IDPO

[34] The interdecadal-decadal Pacific climate oscillation is relatively well recognized after 1860 A.D. [e.g., *Mantua et al.*, 1997; *Power et al.*, 1999; *Hare and Mantua*, 2000; *Folland et al.*, 2002]. However, prior to this time, little is known about interdecadal-decadal scale variability. Before 1860 A.D., our F-T IDPO index shows a regular progression of positive and negative IPO phases (Table 4). The IDPO oscillation appears to have been muted during ~1740 to mid-1750s and also during mid-1680s to mid-1700s. These amplitude changes are observed in both of the coral records that span these intervals (AB and TNI2) (Figure 6) and were abrupt with pronounced IDPO variation before and after each period. This coral δ^{18}O-based IDPO index extends the existing instrumentally derived interdecadal-decadal oscillation indices, e.g., the IPO and the PDO, back to 1650 A.D., providing a reliable reference for the future study of lower-frequency climatic oscillations.

[35] The regularity of the F-T IDPO index indicates that interdecadal-decadal variability in the SPCZ region has been relatively constant over the past 350 years with a mean frequency of ~20 years (variance peaks near 11 and 35 years). This implies some degree of predictability of the

Table 4. Positive and Negative Phases of the IPO and IDPO Index Back to 1650 A.D.[a]

Time Interval	IPO and IPDO Phase
Present to ~2000	Negative
~2000 to early 1980s	Positive
Early1980s to early 1970s	Negative
Early 1970s to early 1960s	Positive
Early 1960s to mid-1940s	Negative
Mid-1940s to early 1920s	Positive
Early 1920s to ~1910	Negative
~1910 to late 1890s	Positive
Late 1890s to early 1890s	Negative
~1890 to mid-1870s	Positive
Mid-1870s to mid-1840s	Negative
Mid-1840s to early 1830s	Positive
Early 1830s to early ~1800s	Negative
Early 1800s to early 1780s	Positive
Early 1780s to ~1770	Negative
~1770 to early 1740s	Positive
Early 1740s to 1720s	Negative
1720s to 1680s	Positive
1680s to late 1660s	Negative
Late 1660s to mid-1650s	Positive

[a]Note that during a positive phase the equatorial central and eastern Pacific is warmer and the SPCZ region is cooler and saltier. During a negative phase the equatorial central and eastern Pacific is cooler and the SPCZ region is warmer and fresher.

IPO/PDO. Following the very strong El Niño of 1997–1998 both the F-T IDPO index and the IPO index began a transition to a negative phase during which the central and eastern equatorial Pacific should be experiencing cooler than average conditions and the subtropics should be warmer than usual. Thus, on the basis of the F-T IDPO regularity and assuming the continued anticorrelation between the F-T IDPO index and the IPO/PDO, the Pacific should be in a La Niña-like mode (negative IPO phase) for the next ~5–10 years then should transition back to a positive IPO phase and more El Niño-like conditions similar to the El Niño-dominated conditions that persisted during the last positive phase of the IPO from ~1976 to the late 1990s. The very strong (1982–1983 and 1997–1998) and prolonged (1990–1994) El Niño events that occurred during this period probably were enhanced by this positive IPO phase. Ignoring changes in the mean state of the Pacific, we suggest that future La Niña events in the next 5–10 years will be stronger because of the additive effects of the IPO phase while the strength of El Niño events will be weakened because of the phase of the IPO.

4.4. F-T IDPO In-Phase in SPCZ and WPWP

[36] Comparison of the IDPO signal at Fiji and Tonga with the IDPO signal in two equatorial Pacific coral $\delta^{18}O$ records at Palmyra [*Cobb et al.*, 2001] and Maiana [*Urban et al.*, 2000] yields a high antiphase correlation (Figure 7c; $r = -0.51$ between Palmyra and F-T IDPO; $r = -0.41$ between Maiana and F-T IDPO). This antiphase correlation is expected because Palmyra and Maiana are both located in an area where SST variability is positively correlated to the IPO while SST in the Fiji and Tonga region is negatively correlated with the IPO (Figure 1) [*Folland et al.*, 2002]. Palmyra (5.9°N, 162.1°W) is located in the center of the tropical Pacific but outside of the WPWP and 1° north of the Niño 3.4 region (shaded box in Figure 1), where ENSO has a larger amplitude than the interdecadal-decadal oscillation [*Cobb et al.*, 2001]. If the coral $\delta^{18}O$ interdecadal-decadal changes at Palmyra are interpreted strictly as temperature (using a range of published coral temperature $\delta^{18}O$ regressions (0.17–0.23‰/°C) [e.g., *Epstein et al.*, 1953; *Dunbar et al.*, 1994; *Gagan et al.*, 1994; *Wellington et al.*, 1996]), the total range of the Palmyra interdecadal-decadal variability (~0.2‰) during 1886–1998 corresponds to ~1°C. This is the same order of magnitude as the interdecadal-decadal variability derived from Niño 3.4 SST anomalies separated by SSA [*Kaplan et al.*, 1998]. This match suggests that the SST variability is the dominant factor affecting the coral $\delta^{18}O$ values in Palmyra over interdecadal-decadal timescales.

[37] In contrast to Palmyra, the $\delta^{18}O$ signal in Maiana records both SST and the $\delta^{18}O_{seawater}$ (directly related to salinity) [*Urban et al.*, 2000]. Maiana (01°N, 173°E) is located 25° west of Palmyra and is near the position of the salinity front on the eastern edge of WPWP [*Donguy*, 1994; *Picaut et al.*, 1996]. Maiana $\delta^{18}O$ interdecadal-decadal variability contains a similar pattern as that at Palmyra and in an opposite phase with F-T IDPO. When a southwest shift of the SPCZ creates locally warmer and fresher conditions (more negative $\delta^{18}O$ value) at Fiji and Tonga, it is accompanied by cooler and saltier conditions at Maiana caused by less rainfall and/or a westward retreat of the equatorial SSS front associated with the WPWP.

[38] The eastward (westward) migration of the warm pool during the El Niño (La Niña) phase of ENSO is well characterized by instrumental data [*Fu et al.*, 1986; *Picaut et al.*, 1996; *Delcroix and McPhaden*, 2002]. Because of the scarcity of long-term instrumental data, the interdecadal-decadal scale displacement of the WPWP eastern salinity front is less well understood. Recently, *Delcroix et al.* [2007] observed the presence of a PDO-like SSS signal in the WPWP, the SPCZ and the Equatorial Cold Tongue during 1970–2003. Figure 8 shows the regression pattern (r values) of precipitation over the interval from 1979 to 2000 [*Xie and Arkin*, 1996] and SST over the interval from 1981 to 2000 [*Reynolds et al.*, 2002] on the SPCZ position index (SPI) [*Folland et al.*, 2002]. Negative correlations (dashed contours) in Figure 8 reflect below average precipitation and SST during positive SPI (and positive phase of the IPO) and positive correlations (thin solid contours) indicate above average precipitation and SST during this positive SPI and IPO phase. From Figure 8, it is clear that precipitation and SST regimes in the Fiji-Tonga (SPCZ) area are reversed from those within the Maiana-Palmyra area of the central equatorial Pacific. This observation agrees with the negative correlation between the five coral composite F-T IDPO index and Maiana-Palmyra, as discussed above.

[39] The precipitation changes at Maiana and Palmyra during a positive phase of the IPO are correlated to the same degree with the SPI (both sites are located between the +0.4 and +0.6 contours in Figure 8). The same result was shown by *Delcroix et al.* [2007, Figure 5] which showed the regression of a 25-month filtered precipitation product on the PDO index. In other words, the precipitation variance on interdecadal-decadal timescales appears to be comparable in

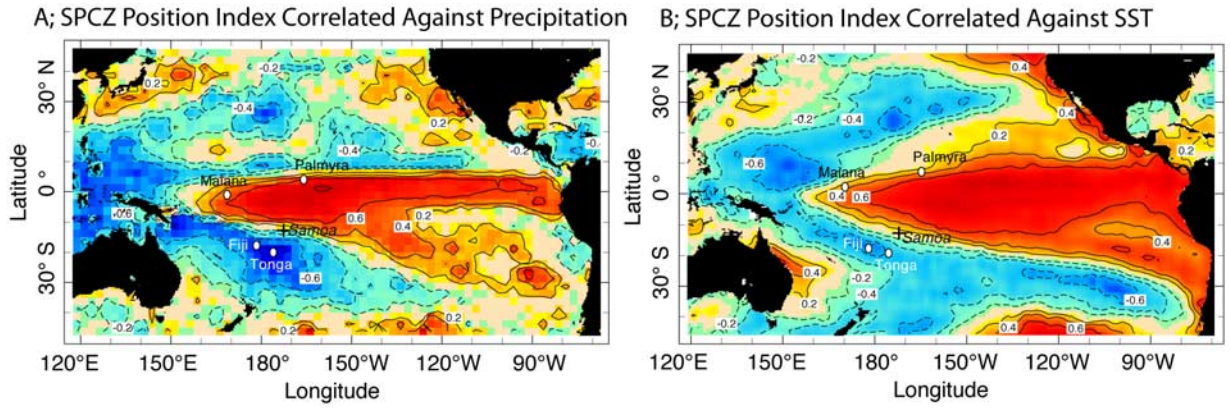

Figure 8. (a) Correlation of SPCZ position index (SPI) [from *Folland et al.*, 2002] against precipitation over the interval from 1979 to 2000 (*R* values). Note that the SPI is based on the air pressure difference between Apia (Samoa) and Suva (Fiji). (b) Correlation of SPCZ position index (SPI) [from *Folland et al.*, 2002] against SST over interval from 1981 to 2000 (*R* values). August–July annual means of precipitation and SST are computed from monthly analyses by *Xie and Arkin* [1996] and *Reynolds et al.* [2002], respectively. The red and orange areas indicate regions with a positive correlation during this time of a positive phase of the IPO index when the equatorial central and eastern Pacific is warmer with enhanced rainfall and the SPCZ region is cooler and saltier. Note the location of our study sites at Fiji and Tonga and that of the coral climate study sites at Maiana [*Urban et al.*, 2000] and Palmyra [*Cobb et al.*, 2001].

these two places. If we assume a near-linear relationship between $\delta^{18}O_{seawater}$, SSS and precipitation in this region, the similar variability of Maiana and Palmyra rainfall on interdecadal-decadal timescales is interesting since variability in coralline $\delta^{18}O$ at Maiana is due to both SST and SSS while at Palmyra it is due mostly to SST. Presently, Maiana is located on the WPWP eastern salinity front while Palmyra is in the center of the equatorial Pacific in a region without a pronounced east-west SSS gradient and away from the WPWP. The migration of the WPWP salinity front will modify SSS near Maiana, but not at Palmyra. An implication of this is that the SSS changes at Maiana are mainly the result of zonal and/or meridional advection, and not precipitation. This is the same conclusion reached by *Delcroix and Picaut* [1998] and *Gouriou and Delcroix* [2002].

[40] Displacements of the SPCZ salinity front can result from local variations in P-E budget or zonal/vertical advection [*Gouriou and Delcroix*, 2002; *Delcroix et al.*, 2007]. In a positive phase of IPO, the westward shift of the SPCZ salinity front could result from a local precipitation shortage or intensified South Equatorial Current. However, when the precipitation deficit increases SSS during a positive IPO, lower SSTs will reduce evaporation, which tend to offset the SSS increase caused by the precipitation shortage. The opposite happens in a negative IPO phase. This increases our confidence that zonal advection is the main contributor to the local SSS change in the SPCZ SSS front region. *Gouriou and Delcroix* [2002] identified westward geostrophic surface current velocity anomalies during El Niño years along 17°S when the SPCZ salinity front shifts westward, and eastward anomalies during La Niña years when the salinity front shifts eastward. This strongly suggests an important role for surface zonal currents in the east-west movement of the SPCZ salinity front on interannual timescales. Because of the lack of long-term instrumental records, we are not able to verify the strengths or velocities of surface ocean current changes and their relationship with IPO, nor can we conclude if the P-E budget or the zonal advection is the dominant factor controlling the SPCZ salinity front shift. If there does exist a local westward surface current anomaly from the cooler and saltier central Pacific Ocean in a positive IPO, it will push the SPCZ salinity front westward and decrease local SST, which agrees with the IPO index (derived from SST data [*Folland et al.*, 2002]) showing cooler than average conditions in a positive IPO. The opposite will occur during negative IPOs, if there exists an eastward surface current anomaly locally that will create warmer and fresher conditions in SPCZ area.

[41] Regardless of the exact mechanism, the opposite displacements of the eastern WPWP and SPCZ salinity fronts are nearly synchronous on interdecadal-decadal timescales, with an average offset between interdecadal-decadal maxima-minima in Maiana and corresponding minima-maxima in the F-T IDPO index of 0.8 years (standard deviation = 1.3 years) (see Figure 7). For Palmyra and the F-T IDPO index, the offset between corresponding interdecadal-decadal minima and maxima is 0.6 years (standard deviation = 1.1 years). The "propagating signal" hypothesis is one of the proposed mechanisms for decadal-interdecadal variability [e.g., *Gu and Philander*, 1997; *Schneider et al.*, 1999; *Luo and Yamagata*, 2001]. These authors argued that water masses subducted in the eastern subtropical south Pacific would travel equator-ward and/or westward along the pycnocline and then upwell along the equator once entrained in the swift equatorial undercurrent. However, the synchronicity of the IDPOs of Maiana and Palmyra (separated by 25° of longitude) indicates little or no time lag for

any IDPO signal traveling along the equator. No time lag also appears between the IDPOs in the equatorial Pacific and in the subtropical Fiji-Tonga region, thus neither region (extratropical or tropical) appears to be leading. Any ocean or ocean-atmosphere coupled model that simulate IPO variation should reflect this opposed yet simultaneous process.

[42] *Burgman et al.* [2008] described the atmospheric processes in the tropical and subtropical Pacific during the 1990s IPO-PDO phase shift. This shift was observed in our five coral composite IDPO index and resulted in the correlation fields shown in Figure 8. Their results suggested an increase in the east-west sea level pressure (SLP) gradient on the equator and intensified Pacific atmospheric circulation during this transition from positive IPO to negative IPO. The same response is also observed on interannual timescales during the transition from El Niño (warm phase of ENSO) to La Niña (cold phase). This could be the reason why we observe similar salinity front movements on both interannual and interdecadal-decadal timescales on the eastern edge of the WPWP and the SPCZ.

5. Conclusions

[43] We have developed a coral δ^{18}O Fiji-Tonga Interdecadal-Decadal Pacific Oscillation (F-T IDPO) index on the basis of annually averaged δ^{18}O time series from five corals collected in Fiji and Tonga (16°49′S–21°02′S, 179°14′E–174°43′W). The F-T IDPO index spans the period 1650–2004 A.D. and has been shown to closely track the IPO and SPI indices. Thus, this index effectively extends our knowledge of interdecadal-decadal ocean-climate variability for ~250 years prior to the instrumental record. The regularity of the F-T IDPO index indicates that interdecadal-decadal variability in the SPCZ region has been relatively constant over the past 350 years with a mean frequency of ~20 years (variance peaks near 11 and 35 years). We note that during ~1740 to the mid-1750s and during the mid-1680s to the mid-1700s the amplitude of the interdecadal-decadal variability diminished sharply. We also observe an anticorrelation with coral δ^{18}O interdecadal-decadal components isolated from other equatorial Pacific coral records at Maiana and Palmyra. This suggests the simultaneous but opposite behavior between the SPCZ and western equatorial Pacific regions. By examining the pattern of precipitation response in Maiana and Palmyra during the last IPO positive phase, we conclude that at interdecadal-decadal timescales, it is the displacement of the salinity front on the eastern edge of WPWP, instead of precipitation changes, that contributes to the SSS variance recorded by coralline δ^{18}O series at Maiana.

[44] Our observations support the results of *Delcroix et al.* [2007] and suggest that the antiphase interdecadal-decadal variations between the equatorial Pacific and the SPCZ region result from the opposing movements of the eastern WPWP and SPCZ salinity fronts. In other words, the interdecadal-decadal eastward expansion (westward contraction) of the WPWP salinity front occurs at the same time as the westward (eastward) shift of the SPCZ salinity front. This antiphase relationship between the SPCZ and eastern WPWP is also observed on seasonal and ENSO timescales [*Gouriou and Delcroix*, 2002]. The WPWP expands eastward during the South Hemisphere winter when the SPCZ retracts; the opposite situation occurs in the South Hemisphere summer when the SPCZ expands southeastward and eastern WPWP retreats westward. In the warm phase of ENSO (El Niño), the eastern WPWP expands while SPCZ contracts and in the cold phase (La Niña), the eastern WPWP retreats westward and SPCZ expands. The synchronous changes of WPWP and SPCZ salinity fronts on interdecadal-decadal timescales could be evidence that atmospheric processes are involved as *Burgman et al.* [2008] conclude. Finally, the regularity of the IPO/PDO over the last several centuries suggests that La Niña events in the next 5–10 years will be stronger because of the additive effects of the IPO phase while the strength of El Niño events will be weakened because of the phase of the IPO.

[45] **Acknowledgments.** For the Fiji component of this research we thank Saimone Tuilaucala (Director of Fisheries) and Aisake Batibasaga (Principal Research Officer) of the Government of Fiji, Ministry of Fisheries and Forests, for supporting this research program. We also thank Jennifer Caselle, David Mucciarone, Tom Potts, Stefan Bagnato, Ove Hoegh-Guldberg, and the J. M. Cousteau Resort in Savasavu (Fiji) for assistance with field sampling. For the Tonga component of this work we gratefully acknowledge "Ulunga Fa" Anunu (Acting Secretary of Fisheries, Ministry of Fisheries in Nuku'alofa) and the Kingdom of Tonga for their support. We are also deeply indebted to the crew of the R. S. V. *Evohe* (Captain Steve Kafka, Kelly McGrath, Allison Paulin, and Greg Brosnan) for their extraordinary assistance in coral core collection in Tonga during November 2004. In Tonga, Sandy Tudhope and Alexa Stolorow also contributed to the collection effort. We thank the two anonymous reviewers and the editor (E. Rohling) for their constructive comments. Earlier phases of this research was supported by NSF grant OCE-0318296 and NOAA grant NA96GP0406 (to B.K.L.), and NSF grant ATM-9619035 and NOAA grant NA96GP0470 (to G.M.W.). This research is most recently supported by NSF grant OCE-0318296 (to B.K.L.) and OCE-0317941 (to A.K.). This is LDEO contribution number 7147. Braddock K. Linsley and Peipei Zhang contributed equally to this work. This paper is dedicated to the memory of Greg Brosnan (Broz). Broz was instrumental in the success of our Tonga November 2004 drilling and helped advance the state of underwater coral drilling. He died tragically in a glider accident in New Zealand in January 2005.

References

Bagnato, S., B. K. Linsley, S. S. Howe, G. M. Wellington, and J. Salinger (2004), Evaluating the use of the massive coral *Diploastrea heliopora* for paleoclimate reconstruction, *Paleoceanography*, *19*, PA1032, doi:10.1029/2003PA000935.

Boyer, T. P., C. Stephens, J. I. Antonov, M. E. Conkright, R. A. Locarnini, T. D. O'Brien, and H. E. Garcia (2002), *World Ocean Atlas 2001* [CD-ROM], vol. 2, *Salinity*, *NOAA Atlas NESDIS*, vol. 50, NOAA, Silver Spring, Md.

Briffa, K. R. (1995), Interpreting high resolution proxy-climate data—The example of dendroclimatology, in *Analysis of Climatic Variability*, edited by H. von Storch and A. Navarra, pp. 77–94, Springer, Berlin, Germany.

Burgman, R. J., A. C. Clement, C. M. Mitas, J. Chen, and K. Esslinger (2008), Evidence for atmospheric variability over the Pacific on decadal timescales, *Geophys. Res. Lett.*, *35*, L01704, doi:10.1029/2007GL031830.

Charles, C. D., D. E. Hunter, and R. G. Fairbanks (1997), Interaction between the ENSO and the Asian Monsoon in a coral record of tropical

climate, *Science*, *277*, 925–928, doi:10.1126/science.277.5328.925.

Cobb, K. M., C. D. Charles, and D. E. Hunter (2001), A central tropical Pacific coral demonstrates Pacific, Indian, and Atlantic decadal climate connections, *Geophys. Res. Lett.*, *28*(11), 2209–2212, doi:10.1029/2001GL012919.

Cobb, K. M., C. D. Charles, H. Cheng, and R. L. Edwards (2003), El Niño/Southern Oscillation and tropical Pacific climate during the last millennium, *Nature*, *424*, 271–276, doi:10.1038/nature01779.

Conkright, M. E. and T. P. Boyer (2002), *World Ocean Atlas 2001: Objective Analyses, Data Statistics, and Figures, CD-ROM Documentation*, 17 pp., Natl. Oceanogr. Data Cent., Silver Spring, Md.

Crowley, T. J., T. M. Quinn, and W. T. Hyde (1999), Validation of coral temperature calibrations, *Paleoceanography*, *14*, 605–615, doi:10.1029/1999PA900032.

Delcroix, T., and M. J. McPhaden (2002), Interannual sea surface salinity and temperature changes in the western Pacific warm pool during 1992–2000, *J. Geophys. Res.*, *107*(C12), 8002, doi:10.1029/2001JC000862.

Delcroix, T., and J. Picaut (1998), Zonal displacements of the western equatorial Pacific fresh pool, *J. Geophys. Res.*, *103*, 1087–1098, doi:10.1029/97JC01912.

Delcroix, T., S. Cravatte, and M. J. McPhaden (2007), Decadal variations and trends in tropical Pacific sea surface salinity since 1970, *J. Geophys. Res.*, *112*, C03012, doi:10.1029/2006JC003801.

Delong, K. L., T. M. Quinn, and F. W. Taylor (2007), Reconstructing twentieth-century sea surface temperature variability in the southwest Pacific: A replication study using multiple coral Sr/Ca records from New Caledonia, *Paleoceanography*, *22*, PA4212, doi:10.1029/2007PA001444.

Donguy, J.-R. (1994), Surface and subsurface salinity in the tropical Pacific ocean: Relations with climate, *Prog. Oceanogr.*, *34*, 45–78, doi:10.1016/0079-6611(94)90026-4.

Dunbar, R. B., G. M. Wellington, M. W. Colgan, and P. W. Glynn (1994), Eastern Pacific sea surface temperature since 1600 A.D.: The δ^{18}O record or climate variability in Galápagos corals, *Paleoceanography*, *9*(2), 291–316, doi:10.1029/93PA03501.

Epstein, S., R. Buchsbaum, H. Lowenstam, and H. C. Urey (1953), Revised carbonate-water isotopic temperature scale, *Geol. Soc. Am. Bull.*, *64*, 1315–1326, doi:10.1130/0016-7606(1953)64[1315:RCITS]2.0.CO;2.

Evans, M. N., A. Kaplan, and M. A. Cane (2000), Intercomparison of coral oxygen isotope data and historical sea surface temperature (SST): Potential for coral-based SST field reconstructions, *Paleoceanography*, *15*, 551–564, doi:10.1029/2000PA000498.

Fairbanks, R. G., M. N. Evans, J. L. Rubenstone, K. Broad, M. D. Moore, and C. D. Charles (1997), Evaluating climate indices and their geochemical proxies measured in corals, *Coral Reefs*, *16*, S93–S100, doi:10.1007/s003380050245.

Folland, C. K., J. A. Renwick, M. J. Salinger, and A. B. Mullan (2002), Relative influences of the Interdecadal Pacific Oscillation and ENSO on the South Pacific Convergence Zone, *Geophys. Res. Lett.*, *29*(13), 1643, doi:10.1029/2001GL014201.

Fu, C. B., H. Diaz, and J. Fletcher (1986), Characteristics of the response of sea surface temperature in the central Pacific associated with the warm episodes of the Southern Oscillation, *Mon. Weather Rev.*, *114*, 1716–1738, doi:10.1175/1520-0493(1986)114<1716:COTROS>2.0.CO;2.

Gagan, M. K., A. R. Chivas, and P. J. Isdale (1994), High-resolution isotopic records from corals using ocean temperature and mass-spawning chronometers, *Earth Planet. Sci. Lett.*, *121*(3–4), 549–558, doi:10.1016/0012-821X(94)90090-6.

Gouriou, Y., and T. Delcroix (2002), Seasonal and ENSO variations of sea surface salinity and temperature in the South Pacific Convergence Zone during 1976–2000, *J. Geophys. Res.*, *107*(C12), 3185, doi:10.1029/2001JC000830.

Gu, D., and S. G. H. Philander (1997), Interdecadal climate fluctuations that depend on exchanges between the tropics and extratropics, *Science*, *275*, 805–807, doi:10.1126/science.275.5301.805.

Hare, S., and N. Mantua (2000), Empirical evidence for North Pacific regime shifts in 1977 and 1989, *Prog. Oceanogr.*, *47*, 103–146, doi:10.1016/S0079-6611(00)00033-1.

Hendy, E. J., M. K. Gagan, J. M. Lough, M. McCulloch, and P. B. deMenocal (2007), Impact of skeletal dissolution and secondary aragonite on trace element and isotopic climate proxies in *Porites* corals, *Paleoceanography*, *22*, PA4101, doi:10.1029/2007PA001462.

Jones, P. D., K. R. Briffa, T. P. Barnett, and S. F. B. Tett (1998), High-resolution palaeoclimatic records for the last millennium: Interpretation, integration and comparison with General Circulation Model control-run temperatures, *Holocene*, *8*(4), 455–471, doi:10.1191/095968398667194956.

Juillet-Leclerc, A., S. Thiria, P. Naveau, T. Delcroix, N. Le Bec, D. Blamart, and T. Corrège (2006), SPCZ migration and ENSO events during the 20th century as revealed by climate proxies from a Fiji coral, *Geophys. Res. Lett.*, *33*, L17710, doi:10.1029/2006GL025950.

Kaplan, A., M. Cane, Y. Kushnir, A. Clement, M. Blumenthal, and B. Rajagopalan (1998), Analyses of global sea surface temperature 1856–1991, *J. Geophys. Res.*, *103*(18), 567–589.

LeGrande, A. N., and G. A. Schmidt (2006), Global gridded data set of the oxygen isotopic composition in seawater, *Geophys. Res. Lett.*, *33*, L12604, doi:10.1029/2006GL026011.

Linsley, B. K., R. B. Dunbar, G. M. Wellington, and D. A. Mucciarone (1994), A coral based reconstruction of Intertropical Convergence Zone variability over Central America since 1707, *J. Geophys. Res.*, *99*(C5), 9977–9994, doi:10.1029/94JC00360.

Linsley, B. K., R. G. Messier, and R. B. Dunbar (1999), Assessing between-colony oxygen isotope variability in the coral *Porites lobata* at Clipperton Atoll, *Coral Reefs*, *18*(1), 13–27, doi:10.1007/s003380050148.

Linsley, B. K., G. M. Wellington, and D. P. Schrag (2000), Decadal sea surface temperature variability in the subtropical Pacific from 1726 to 1997 A. D, *Science*, *290*, 1145–1148, doi:10.1126/science.290.5494.1145.

Linsley, B. K., G. M. Wellington, D. P. Schrag, L. Ren, M. J. Salinger, and A. W. Tudhope (2004), Geochemical evidence from corals for changes in the amplitude and spatial pattern of South Pacific interdecadal climate variability over the last 300 years, *Clim. Dyn.*, *22*, 1–11, doi:10.1007/s00382-003-0364-y.

Linsley, B. K., A. Kaplan, Y. Gouriou, J. Salinger, P. B. deMenocal, G. M. Wellington, and S. S. Howe (2006), Tracking the extent of the South Pacific Convergence Zone since the early 1600s, *Geochem. Geophys. Geosyst.*, *7*, Q05003, doi:10.1029/2005GC001115.

Lough, J. M. (2004), A strategy to improve the contribution of coral data to high resolution, *Palaeogeogr. Palaeoclimatol. Palaeoecol.*, *204*(1–2), 115–143, doi:10.1016/S0031-0182(03)00727-2.

Luo, J.-J., and T. Yamagata (2001), Long-term El Nino-southern oscillation (ENSO)-like variation with special emphasis on the South Pacific, *J. Geophys. Res.*, *106*, 22,211–22,227, doi:10.1029/2000JC000471.

Mann, M. E., and J. Park (1994), Global-scale modes of surface temperature variability on interannual to century timescales, *J. Geophys. Res.*, *99*(D12), 25,819–25,834, doi:10.1029/94JD02396.

Mantua, N., S. Hare, Y. Zhang, J. Wallace, and R. Francis (1997), A Pacific interdecadal climate oscillation with impacts on salmon productions, *Bull. Am. Meteorol. Soc.*, *78*, 1069–1079, doi:10.1175/1520-0477(1997)078<1069:APICOW>2.0.CO;2.

Minobe, S., T. Manabe, and A. Shouji (2002), Maximal wavelet filter and its application to didecadal oscillation over the Northern Hemisphere through the twentieth century, *J. Clim.*, *15*(9), 1064–1075, doi:10.1175/1520-0442(2002)015<1064:MWFAIA>2.0.CO;2.

Morimoto, M., O. Abe, H. Kayanne, N. Kurita, E. Matsumoto, and Y. Yoshida (2002), Salinity records for the 1997–98 El Niño from western Pacific corals, *Geophys. Res. Lett.*, *29*(11), 1540, doi:10.1029/2001GL013521.

Müller, A., M. K. Gagan, and M. T. McCulloch (2001), Early marine diagenesis in corals and geochemical consequences for paleoceanographic reconstructions, *Geophys. Res. Lett.*, *28*, 4471–4474, doi:10.1029/2001GL013577.

Pätzold, J. (1984), Growth rhythms recorded in stable isotopes and density bands in the reef coral *Porites lobata* (Cebu, Philippines), *Coral Reefs*, *3*(2), 87–90, doi:10.1007/BF00263758.

Picaut, J., M. Ioualalen, C. Menkes, T. Delcroix, and M. McPhaden (1996), Mechanism of the zonal displacements of the Pacific Warm Pool: Implications for ENSO, *Science*, *274*, 1486–1489, doi:10.1126/science.274.5292.1486.

Power, S., T. Casey, C. Folland, A. Coleman, and V. Metha (1999), Interdecadal modulation of the impact of ENSO on Australia, *Clim. Dyn.*, *15*, 319–324, doi:10.1007/s003820050284.

Priess, K., T. Le Campion-Alsumard, S. Golubic, F. Gadel, and B. A. Thomassin (2000), Fungi in corals: Black bands and density banding of *Porites lutea* and *P. lobata* skeleton, *Mar. Biol.*, *136*, 19–27, doi:10.1007/s002270050003.

Reynolds, R. W., and T. M. Smith (1994), Improved global sea surface temperature analyses using optimum interpolation, *J. Clim.*, *7*(6), 929–948, doi:10.1175/1520-0442(1994)007<0929:IGSSTA>2.0.CO;2.

Reynolds, R. W., N. A. Rayner, T. M. Smith, D. C. Stokes, and W. Wang (2002), An improved in-situ and satellite SST Analysis for climate, *J. Clim.*, *15*, 1609–1625, doi:10.1175/1520-0442(2002)015<1609:AIISAS>2.0.CO;2.

Salinger, M. J., R. E. Basher, B. B. Fitzharris, J. E. Hay, P. D. Jones, J. P. Macvergh, and I. Schmidely-Leleu (1995), Climate trends in the south-west Pacific, *Int. J. Climatol.*, *15*(3), 285–302, doi:10.1002/joc.3370150305.

Schneider, N., S. Venzke, A. J. Miller, D. W. Pierce, T. Barnett, C. Deser, and M. Latif (1999), Pacific thermocline thermocline bridge revisited, *Geophys. Res. Lett.*, *26*, 1329–1332, doi:10.1029/1999GL900222.

Tudhope, A. W., G. B. Shimmield, C. P. Chilcott, M. Jebb, A. E. Fallick, and A. N. Dalgleish (1995), Recent changes in climate in the far western equatorial Pacific and their relationship to the Southern Oscillation: Oxygen isotope records from massive corals, Papua New Quinea, *Earth Planet. Sci. Lett.*, *136*, 575–590, doi:10.1016/0012-821X(95)00156-7.

Urban, F. E., J. E. Cole, and J. T. Overpeck (2000), Influence of mean climate change on climate variability from a 155-year tropical Pacific coral record, *Nature*, *407*, 989–993, doi:10.1038/35039597.

Vautard, R., and M. Ghil (1989), Singular spectrum analysis in nonlinear dynamics, with applications to Paleoclimatic time series, *Physica D*, *35*, 395–424, doi:10.1016/0167-2789(89)90077-8.

Vautard, R., P. Yiou, and M. Ghil (1992), Singular-spectrum analysis: A toolkit for short, noisy chaotic signals, *Physica D*, *58*, 95–126, doi:10.1016/0167-2789(92)90103-T.

Wellington, G. M., R. B. Dunbar, and G. Merlen (1996), Calibration of stable oxygen isotope signatures in Galapagos corals, *Paleoceanography*, *11*, 467–480, doi:10.1029/96PA01023.

Wigley, T. M. L., K. R. Briffa, and P. D. Jones (1984), On the average value of correlated time-series, with applications in dendroclimatology and hydrometeorology, *J. Clim. Appl. Meteorol.*, *23*(2), 201–213, doi:10.1175/1520-0450(1984)023<0201:OTAVOC>2.0.CO;2.

Xie, P., and P. A. Arkin (1996), Analyses of global monthly precipitation using gauge observations, satellite estimates and numerical model predictions, *J. Clim.*, *9*, 840–858, doi:10.1175/1520-0442(1996)009<0840:AOGMPU>2.0.CO;2.

S. S. Howe, B. K. Linsley, and P. Zhang, Department of Earth and Atmospheric Sciences, University at Albany, State University of New York, Albany, NY 12222, USA. (showe@albany.edu; blinsley@albany.edu; zhang_pei_pei@hotmail.com)

A. Kaplan, Lamont-Doherty Earth Observatory, Columbia University, P.O. Box 1000, 61 Route 9W, Palisades, NY 10964, USA. (alexeyk@ldeo.columbia.edu)

G. M. Wellington, Department of Biology and Biochemistry, University of Houston, 4800 Calhoun Road, Houston, TX 77004, USA.